

Sulfur Substituted LiFePO₄/C with Improved Rate Performance for Lithium Ion Batteries

Tao Yu⁺, Zhao Wang⁺, Yao Fu, Yachao Xiong, Shiyong Guan^{*}

School of Materials Science and Engineering, East China University of Science and Technology, Mei Long Road 130, Shanghai 200237, P.R. China

[+] These authors contributed equally to this work.

*E-mail: syguan@ecust.edu.cn

Received: 27 April 2016 / Accepted: 26 May 2016 / Published: 4 June 2016

Sulfur substituted LiFePO₄/C sample was successfully synthesized by solid state method. The importation of sulfur ion can slightly increase the lattice parameters of LiFePO₄ while maintaining the original orthorhombic olivine structure. Electrochemical tests show the rate capacity of sulfur substituted LiFePO₄/C was significantly improved comparing with LiFePO₄/C. The improvement of the rate performance is attributed to the importation of sulfur ion which may expand the Li⁺ ion diffusion pathway to facilitate charge transfer and Li⁺ ion diffusion. The results indicate that sulfur substitution can be an effective approach to improve the electrochemical performance of LiFePO₄/C cathode materials for lithium ion batteries.

Keywords: Sulfur substitution; Lithium iron phosphate; Solid state reaction; Rate performance.

1. INTRODUCTION

Lithium ion batteries (LIBs) greatly propel the rapid development of energy storage, electric vehicles and hybrid electric vehicles due to its superiorities of high energy density, high voltage, long cycle life and environmental friendliness [1, 2]. As a crucial portion of LIBs, cathode materials have undoubtedly become one of the challenges to further improve the electrochemical performance of batteries [3]. Comparing with conventional cathode materials such as layer LiMO₂ (M= Co, Ni, Mn) and spinel LiMn₂O₄, olivine LiFePO₄ shows great advantages of abundant material supply, low cost, non-toxic, and environmentally benign [4, 5]. Unfortunately, two fatal weaknesses—low electronic conductivity ($\sim 10^{-9}$ S cm⁻¹) and poor Li⁺ ionic conductivity ($\sim 10^{-14}$ cm² s⁻¹) seriously hinder the application of LiFePO₄ material in the field of power lithium ion batteries [6].

Aiming at such problems, numerous approaches have been proposed, such as coating with carbon-base materials or stable Li^+ ion conductors [7-9], reducing the particle size [10-12] and addition of dispersion metal powder [13]. Recently, substitution of external ions in the bulk materials has been covered to improve ionic and electronic conductivity as well [14-19], and these ions include Al^{3+} , Cr^{3+} , B^{3+} , Cu^{2+} , F^- and S^{2-} . For instance, Wang et al. [20] synthesized bivalent cation (Ni^{2+} , Co^{2+} , Mg^{2+}) substituted LiFePO_4 in Fe-sites and found the target products show improved rate performance and cyclic stability. The results indicated that electronic conductivity increased by two orders of magnitude and the Li-O interaction was weakened by ions substitution which can facilitate Li^+ ionic mobility. Sun et al. [21] prepared Cl^- substituted LiFePO_4/C cathode materials using a carbothermal reduction route and found the specific capacity of target product was improved to be $\sim 90 \text{ mAh g}^{-1}$ at the rate of 20 C. They proposed the introduction of Cl^- ions may elongate the interatomic distances of Li-O and shorten the lengths of P-O to optimize Li^+ ion diffusion and stabilize the framework of LiFePO_4 .

Owing to the advantages of foreign ions substitution on improving the ionic conductivity and intrinsic electronic conductivity of LiFePO_4 material, we employed solid-state reaction to synthesis sulfur substituted LiFePO_4 composites with carbon coating. Sulfur is appropriate for dopant of cathode materials with the merits of abundance, availability, and nontoxicity [22]. In addition, the solid-state reaction is appropriate for large-scale synthesis due to its simplicity procedure [23]. Results indicate that the substitution of sulfur ion can efficiently facilitate charge and Li^+ ion transfer, and thus improve the electrochemical performance of LiFePO_4 , especially at high current density. The optimum parameters in the process of synthesis of sulfur substituted LiFePO_4/C are discussed in detail.

2. EXPERIMENTAL

Sulfur substituted LiFePO_4/C materials were prepared using Li_2S , Li_2CO_3 , $\text{FeC}_2\text{O}_4 \cdot 2\text{H}_2\text{O}$, $\text{NH}_4\text{H}_2\text{PO}_4$ and sucrose as raw materials via solid-state route. A general procedure of the experiment is described as follows. A mixture of $\text{FeC}_2\text{O}_4 \cdot 2\text{H}_2\text{O}$ and $\text{NH}_4\text{H}_2\text{PO}_4$ in stoichiometric ratio was thoroughly ball-milled for 10 h with 10 wt% sucrose as carbon source and then dried at $60 \text{ }^\circ\text{C}$ for 24 h in a vacuum oven. Subsequently, the mixture was heat treated at $350 \text{ }^\circ\text{C}$ for 6 h in a tubular furnace (the heating speed was $5 \text{ }^\circ\text{C min}^{-1}$) under pure nitrogen atmosphere to obtain precursor. After that, the mixture of Li_2S and Li_2CO_3 was added into the precursor, and then was thoroughly ball-milled again. At last, the target products were achieved by sintering above mixture in a tubular furnace at $600\text{--}750 \text{ }^\circ\text{C}$ (the heating rate was $5 \text{ }^\circ\text{C min}^{-1}$) for 10 h under pure nitrogen atmosphere. In order to optimize the sintering temperature and the addition content of Li_2S , different samples have been prepared and the corresponding products are denoted as $\text{S}_x\text{-LFP/C-y}$, where x and y represent the addition content of Li_2S and the sintering temperature, respectively. The molar ratios of $\text{Li}_2\text{S}:\text{Li}_2\text{CO}_3$ were varied as follows: 1:3, 1:1, 3:1, 1:0 and the corresponding products are denoted as $\text{S}_1\text{-LFP/C}$, $\text{S}_2\text{-LFP/C}$, $\text{S}_3\text{-LFP/C}$ and $\text{S}_4\text{-LFP/C}$, respectively. Moreover, the sintering temperature was varied as 600, 650, 700 and $750 \text{ }^\circ\text{C}$. For comparison, LiFePO_4/C without substitution which is named as LFP/C was obtained using the similar procedure in absence of Li_2S .

The crystal structure of sulfur substituted LiFePO_4/C composites was identified by X-ray diffraction (XRD, D/MAX 2550VB/PC, Rigaku, Japan) with a $\text{Cu K}\alpha$ radiation. The PDF standard card (JCPDS #83-2092) was used to compare with the XRD patterns of the samples prepared. The morphology was characterized by scanning electron microscopy (SEM, JSM-6360LV, JEOL, Japan) and transmission electron microscopy (TEM, JEM-1400, JEOL, Japan). Energy dispersive spectrometer (EDS, Falcon, EDAX, USA) was performed to identify the composition of the samples.

The electrochemical performance of the samples was achieved by using a CR2016 type cell. The cathode film was composed of 80 wt% active material (LiFePO_4/C or sulfur substituted LiFePO_4/C), 10 wt% acetylene black and 10 wt% polyvinylidene fluoride. Metallic lithium was used as the counter electrode, 1 M LiPF_6 in a 1:1 v/v mixture of ethylene carbonate (EC) and dimethyl carbonate (DMC) served as electrolyte, and Celgard3025 type films acted as separator. At last, button cells were fabricated in a glove box under high-pure argon atmosphere. Galvanostatic charge/discharge measurements were performed in a Land CT2001A battery tester (Neware, Shenzhen, China) with the cut-off voltage of 2.5 V and 4.2 V under different rates at room temperature. The electrochemical impedance spectroscopy (EIS) was performed on an electrochemical workstation CHI660D (Chenhua, Shanghai, China) with the frequency range of 10^{-3} to 10^6 Hz and the potential amplitude of 5 mV.

3. RESULTS AND DISCUSSION

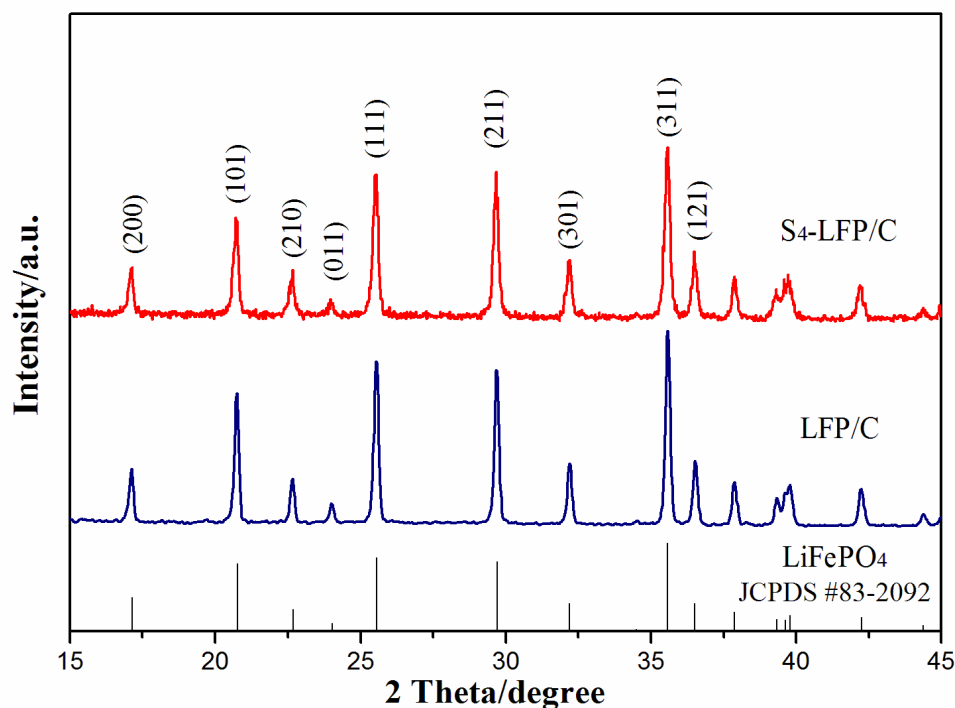


Figure 1. XRD patterns of (a) LiFePO_4 (JCPDS #83-2092), (b) LFP/C and (c) $\text{S}_4\text{-LFP/C}$ (LFP/C and $\text{S}_4\text{-LFP/C}$ were prepared with the same sintering temperature of 700 °C in absence of Li_2S and Li_2CO_3 , respectively).

X-ray diffraction was introduced to confirm the effect of sulfur substitution on the olivine structure of LiFePO_4 . Fig. 1 shows the XRD patterns of pristine LiFePO_4 , LFP/C, and $\text{S}_4\text{-LFP/C}$ samples. All peaks on the curve of the obtained LFP/C and $\text{S}_4\text{-LFP/C}$ can be clearly indexed to an ordered orthorhombic olivine structure with a space group Pmnb (JCPDS #83-2092), indicating LiFePO_4 phase has been successfully synthesized and sulfur substitution does not destroy the structure of LiFePO_4 [24, 25]. Besides, the diffraction peaks relating to Li_2S material were not detected in the patterns of LFP/C and $\text{S}_4\text{-LFP/C}$, implying Li_2S has participated in the reaction completely. Furthermore, obvious diffraction peaks of carbon were not observed, attributing to the amorphous phase of carbon [26].

Table 1. Lattice parameters of LiFePO_4 (JCPDS #83-2092), LFP/C and $\text{S}_4\text{-LFP/C}$.

	a(Å)	b(Å)	c(Å)	Volume(Å ³)
LiFePO_4 (JCPDS #83-2092)	10.334	6.01	4.693	291.47
LFP/C	10.32046	6.00459	4.69286	290.82
$\text{S}_4\text{-LFP/C}$	10.34877	6.02163	4.7033	293.09

For further calculation, the lattice parameters of LFP/C and $\text{S}_4\text{-LFP/C}$ were achieved based on XRD patterns and the results are shown in Table 1. It is apparently seen that the obtained samples exhibit exactly the similar value with that of LiFePO_4 (JCPDS #83-2092).

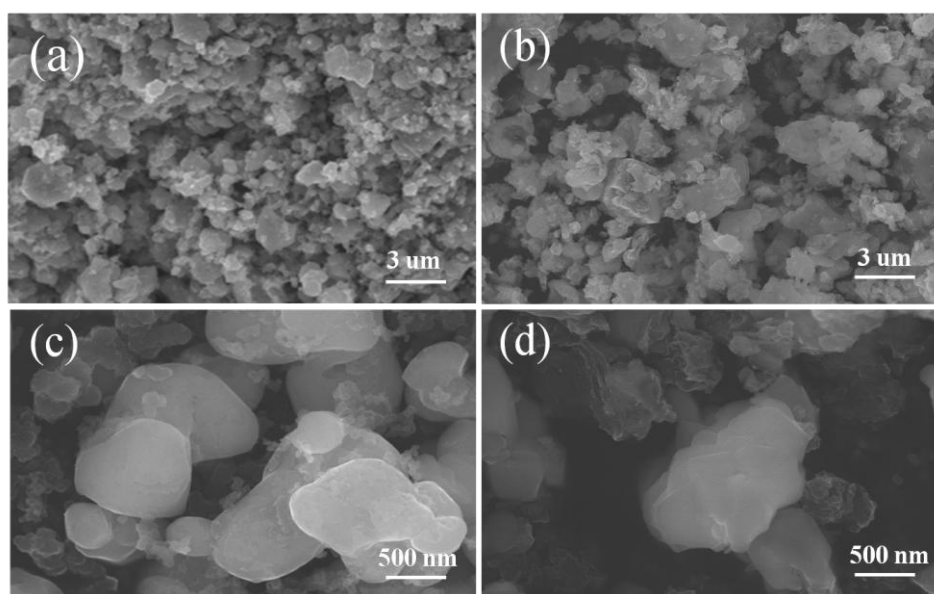


Figure 2. SEM images of (a) LFP/C and (b) $\text{S}_4\text{-LFP/C}$, and the following images of (c) and (d) represent the amplification maps of LFP/C and $\text{S}_4\text{-LFP/C}$, respectively.

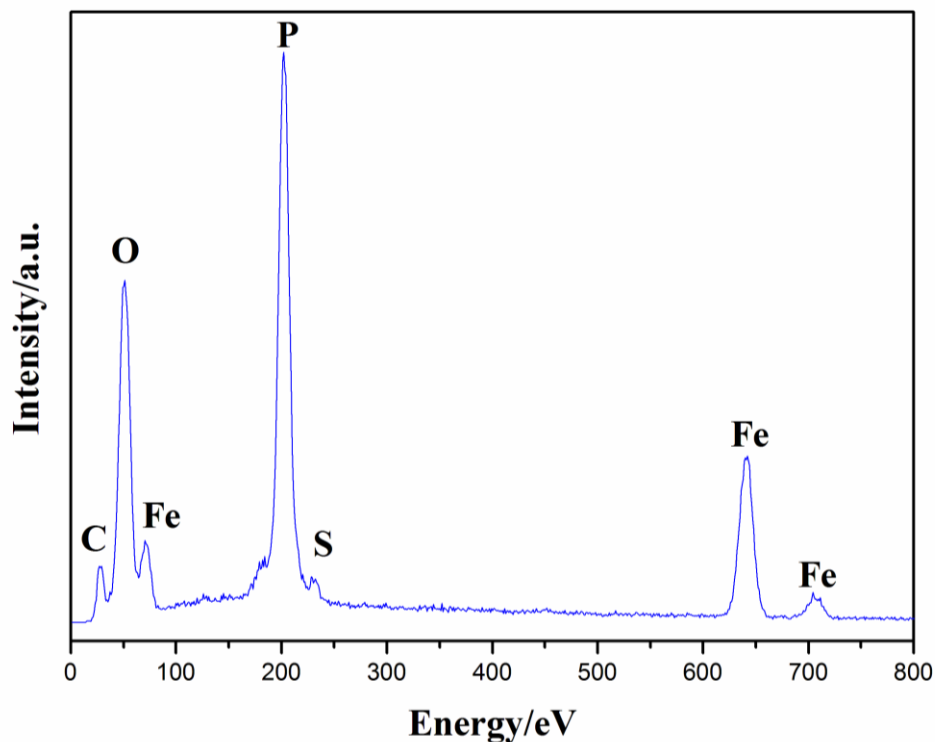


Figure 3. EDS spectrum of S_4 -LFP/C composite.

Contrasting with LFP/C, the lattice parameters of a, b and c axis in S_4 -LFP/C composite increase 0.27%, 0.28% and 0.22%, respectively, and the lattice volume increases 0.78% as well, implying sulfur ion has been successfully introduced into the internal structure of $LiFePO_4$. The slightly variation of lattice parameters probable be attributed to the substitution of O-sites in $LiFePO_4$ with sulfur ion, which has larger ionic radius than oxygen ion.

In order to confirm the influence of sulfur substitution on morphology of $LiFePO_4$, SEM and TEM were performed to observe the morphology of the obtained samples. Fig. 2 shows the SEM images of LFP/C and S_4 -LFP/C. From the images of Fig. 2a and 2b, it is obvious that both of substituted and unsubstituted $LiFePO_4$ /C have the similar morphology and homogeneous distribution particles. In the amplification images of Fig. 2c and 2d, the particle sizes of LFP/C and S_4 -LFP/C samples were similarly 1 μm , indicating the substitution of sulfur ion in $LiFePO_4$ does not damage the morphology and dimension of $LiFePO_4$ particles. Fig. 3 shows the EDS spectrum of S_4 -LFP/C composite. The peak of sulfur element on EDS spectrum can be observed, despite the intensity of those peaks are weaker than that of other main elements, such as Fe, O and P. Consistent with the results shown in XRD pattern, sulfur ions have successfully permeated into the bulk of $LiFePO_4$ matrix.

Fig. 4 shows the TEM images of LFP/C and S_4 -LFP/C. From those images, LFP/C and S_4 -LFP/C particles are surrounded by carbon granule which exhibits smoke-like shape and uniformly attaches to the surface of active materials. It is considered that the carbon coating plays a role as 'a bridge' to accelerate charge transfer among $LiFePO_4$ particles, and the incompact structure with some voids is beneficial for electrolyte infiltration and storage resulting in enhanced rate performance of the

sample [23].

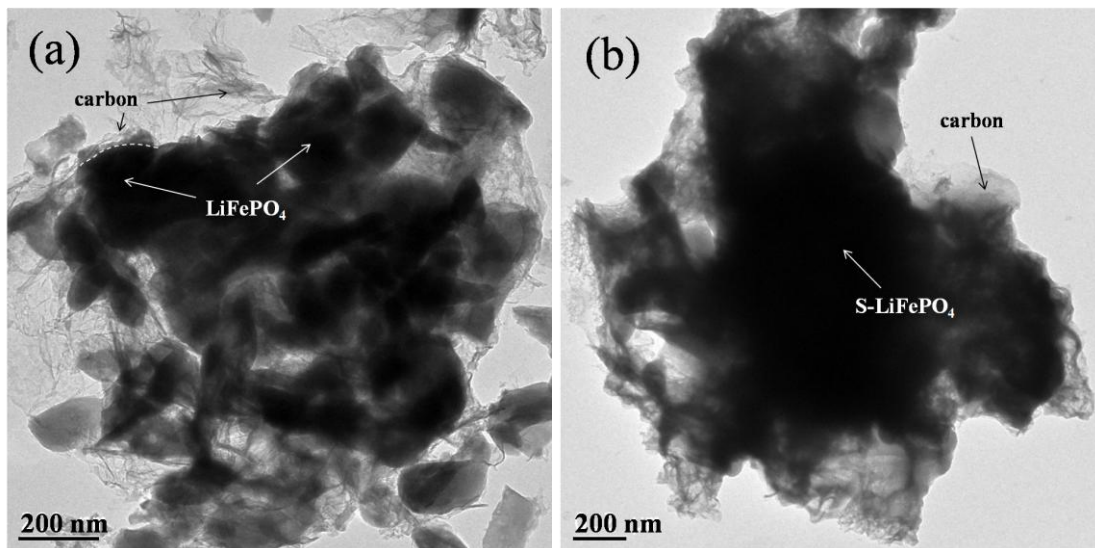


Figure 4. TEM images of (a) LFP/C and (b) S₄-LFP/C.

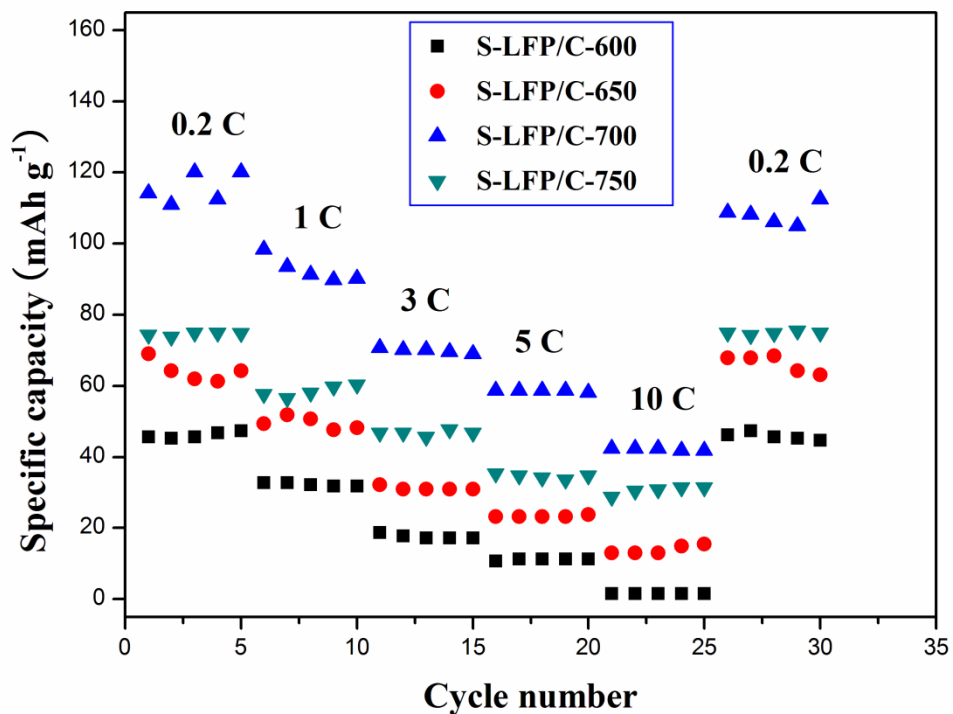


Figure 5. The rate capacity of S-LFP/C samples at different sintering temperatures (600, 650, 700 and 750 °C, respectively) with Li₂S as Li source.

The rate performance of LiFePO_4/C and sulfur substituted LiFePO_4/C was investigated by galvanostatic cycling at various rates and the optimization of synthetic route was studied in detail as follows.

Fig. 5 shows the specific capacity of S-LFP/C samples which were synthesized at different sintering temperatures ($600\sim 750\text{ }^\circ\text{C}$) at various rates. From Fig. 5, it can be seen that S-LFP/C-700 sintered under $700\text{ }^\circ\text{C}$ possesses the highest discharge capacity at different current densities, indicating $700\text{ }^\circ\text{C}$ is more suitable for the preparation of sulfur substituted LiFePO_4/C . The reasonable interpretation may be that materials with heat treatment at low temperature develop an imperfect crystalline structure, while the crystallization velocity is too fast under high heat treatment temperature leading to crystal defects. Therefore, the heat treatment with too low or too high temperature is adverse to the electrochemical performance of materials.

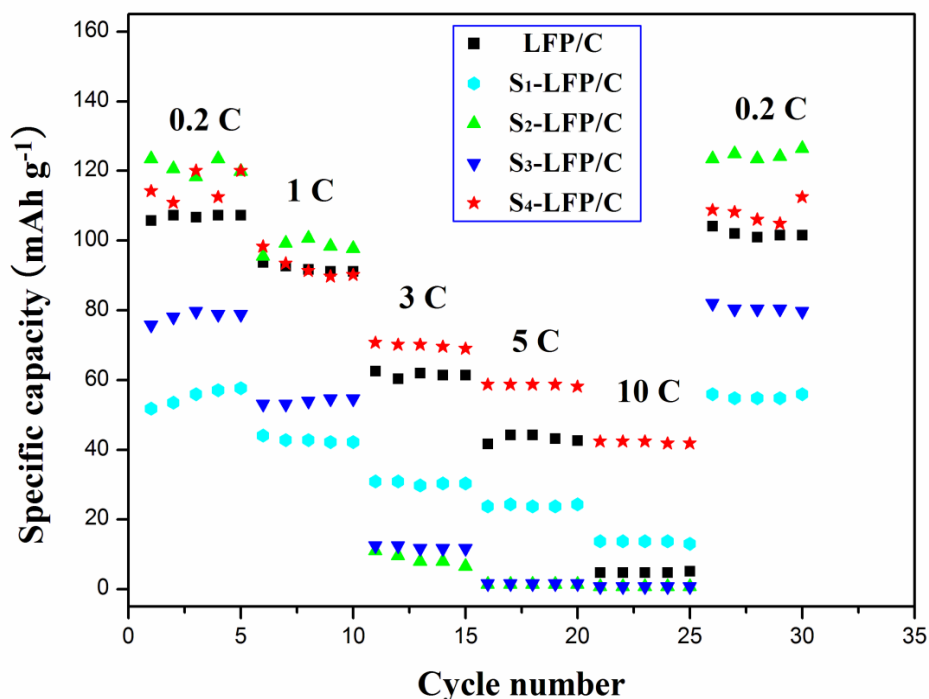


Figure 6. The rate capacity of LFP/C and S_{1-4} -LFP/C samples with the molar ratios of $\text{Li}_2\text{S}:\text{Li}_2\text{CO}_3 = 1:3, 1:1, 3:1, 1:0$, respectively, with the same sintering temperature of $700\text{ }^\circ\text{C}$.

Afterwards, various samples with different addition amount of Li_2S were prepared at the same synthetic process with the sintering temperature at $700\text{ }^\circ\text{C}$. Fig. 6 shows the discharge specific capacity of various sulfur substituted LiFePO_4/C samples at different rates. It can be clearly seen that S_4 -LFP/C sample synthesized by adding Li_2S completely without Li_2CO_3 has a similar discharge specific capacity at low rate (0.2 and 1 C) comparing with some other substituted materials, while owns the best electrochemical performance at high current density (3, 5, and 10 C). Therefore, it is an optimal choice for Li_2S completely replacing Li_2CO_3 as Li and S source. At the same time, the initial specific capacity of S_4 -LFP/C and LFP/C are 114.1 and 105.7 mA h g^{-1} at the rate of 0.2 C, respectively. After

increasing current density to 5 C, the specific capacity of S₄-LFP/C and LFP/C decrease to 58.7 mA h g⁻¹ (the capacity retention of 51.4%) and 41.7 mA h g⁻¹ (39.4%), respectively. At 10 C current rate, the specific capacity of S₄-LFP/C and LFP/C are 42.39 mA h g⁻¹ (37.1%) and 4.7 mA h g⁻¹ (4.4%), respectively. The improved electrochemical performance mainly attributes to the substitution of sulfur element in LiFePO₄ matrix. It is well known that the poor Li⁺ ion conductivity in LiFePO₄ particles due to Li⁺ ion preferentially diffuses along with one-dimension (010) channel in the lattice of LiFePO₄, which is easy to hinder the movement of Li⁺ ion especially at high current density [27]. The importation of sulfur ion may expand the Li⁺ ion diffusion pathway due to the larger ionic radius of S²⁻ (0.173 nm) against that of O²⁻ (0.132 nm) [28]. Simultaneously, it will become easier for the migration of Li⁺ ion as well, because the electronegativity of sulfur is lower than that of oxygen [29]. In addition, ion substitution has the ability to enhance the intrinsic electronic conductivity which was proved on the perspective of experiment and density-functional theory [16, 30].

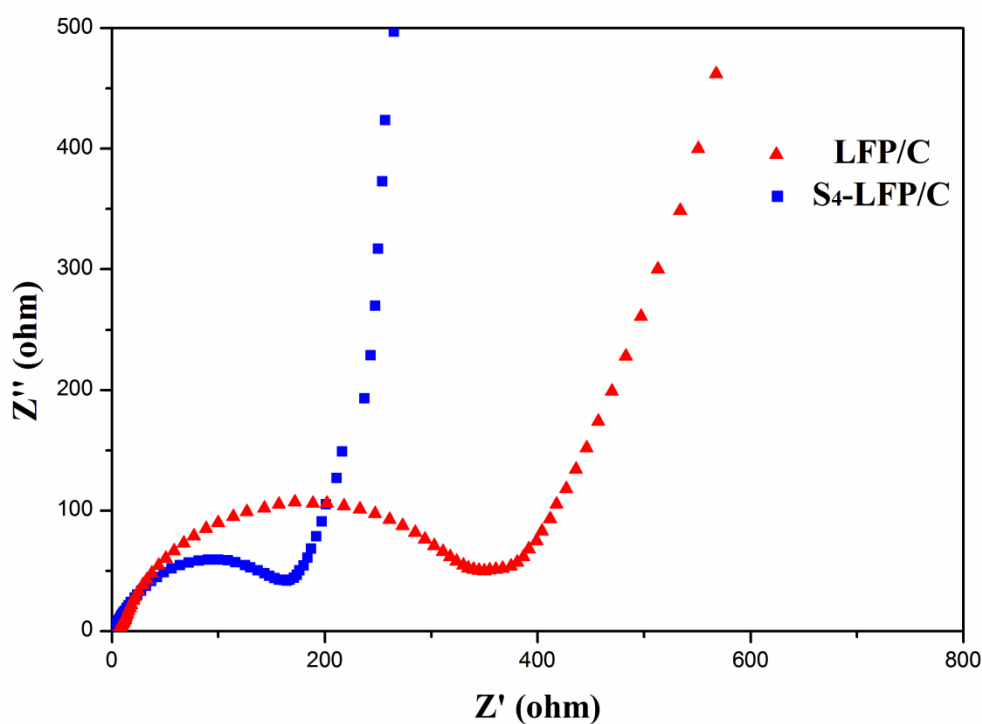


Figure 7. Electrochemical impedance spectroscopy (EIS) of LFP/C and S₄-LFP/C

In order to analysis the effect of sulfur substitution on electrochemical kinetic performance of LiFePO₄/C cathodes, EIS spectra were performed. Fig. 7 shows the EIS spectra of LFP/C and S₄-LFP/C samples. It can be seen that EIS spectrum is constitutive of a semicircle in high frequency area and a sloping line in low frequency area. The semicircle indicates the charge transfer resistance (R_{ct}) and the sloping line represents the Warburg impedance (Z_w) reflecting the diffusion of Li⁺ ion at the electrode/electrolyte interface [9, 31]. As shown in Fig. 7, the semicircle diameter of S₄-LFP/C is smaller than that of LFP/C, indicating S₄-LFP/C sample owns the lower R_{ct} value. The slope of the straight line of S₄-LFP/C is bigger than that of LFP/C, representing S₄-LFP/C has smaller Warburg

impedance and better Li⁺ ion transport property [32]. The improved performance of the charge transfer and Li⁺ ion diffusion are greatly attributed to the substitution of sulfur ion in the bulk of LiFePO₄.

4. CONCLUSIONS

In this paper, we successfully synthesize sulfur substituted LiFePO₄ samples with carbon coating using solid state method. The experiment results show that the optimum synthetic procedure of sulfur substituted LiFePO₄/C material is that using Li₂S completely without Li₂CO₃ as raw material and setting sintering temperature at 700 °C. The substitution of sulfur ion would not damage the orthorhombic olivine structure of LiFePO₄ and has the ability to expand the Li⁺ ion diffusion pathway. Electrochemical performance measurements show the substitution of sulfur ion can significantly improve the discharge capacity of LiFePO₄ materials by reducing the internal Li⁺ ion transmission impedance at high rate currents. This is mainly due to the sulfur element doping in O-sites of LiFePO₄ crystal lattice to provide greater Li⁺ transmission channel. In conclusions, sulfur substitution can be an effective approach to improve the electrochemical performance of LiFePO₄/C cathode materials for lithium ion batteries.

References

1. T.H. Kim, J.S. Park, S.K. Chang, S. Choi, J.H. Ryu and H.K. Song, *Adv. Energy Mater.*, 2 (2012) 860.
2. B. Scrosati and J. Garche, *J. Power Sources*, 195 (2010) 2419.
3. J.W. Fergus, *J. Power Sources*, 195 (2010) 939.
4. A.K. Padhi, K.S. Nanjundaswamy and J.B. Goodenough, *J. Electrochem. Soc.*, 144 (1997) 1188.
5. W.J. Zhang, *J. Power Sources*, 196 (2011) 2962.
6. C.S. Wang and J. Hong, *Electrochem. Solid-State Lett.*, 10 (2007) A65.
7. J. Gim, J. Song, D. Nguyen, M.H. Alfaruqi, S. Kim, J. Kang, A.K. Rai, V. Mathew and J. Kim, *Ceram. Int.*, 40 (2014) 1561.
8. Q.Y. Li, F.H. Zheng, Y.G. Huang, X.H. Zhang, Q. Wu, D.J. Fu, J.J. Zhang, J.C. Yin and H.Q. Wang, *J. Mater. Chem. A*, 3 (2015) 2025.
9. G.Q. Tan, F. Wu, L. Li, R.J. Chen and S. Chen, *J. Phys. Chem. C*, 117 (2013) 6013.
10. D.H. Kim and J. Kim, *Electrochem. Solid-State Lett.*, 9 (2006) A439.
11. M.H. Lee, J.Y. Kim and H.K. Song, *Chem. Commun.*, 46 (2010) 6795.
12. C. Sun, S. Rajasekhara, J.B. Goodenough and F. Zhou, *J. Am. Chem. Soc.*, 133 (2011) 2132.
13. F. Croce, A.D. Epifanio, J. Hassoun, A. Deptula, T. Olczac and B. Scrosati, *Electrochem. Solid-State Lett.*, 5 (2002) A47.
14. S.Y. Chung, J.T. Bloking and Y.M. Chiang, *Nat. Mater.*, 1 (2002) 123.
15. S.M. Zheng, X. Wang, X. Huang and C.H. Liu, *Ceram. Int.*, 38 (2012) 4391.
16. C. Ban, W.J. Yin, H. Tang, S.H. Wei, Y. Yan and A.C. Dillon, *Adv. Energy Mater.*, 2 (2012) 1028.
17. R. Trócoli, S. Franger, M. Cruz, J. Morales and J. Santos-Peña, *Electrochim. Acta*, 135 (2014) 558.
18. Z.P. Ma, Y.Q. Fan, G.J. Shao, L. Wang, J.J. Song, G.L. Wang and T.T. Liu, *Electrochim. Acta*, 139 (2014) 256.
19. S.B. Lee, S.H. Cho, V. Aravindan, H.S. Kim and Y.S. Lee, *Bull. Korean Chem. Soc.*, 30 (2009) 2223.
20. D.Y. Wang, H. Li, S.Q. Shi, X.J. Huang and L.Q. Chen, *Electrochim. Acta*, 50 (2005) 2955.

21. C.S. Sun, Y. Zhang, X.J. Zhang and Z. Zhou, *J. Power Sources*, 195 (2010) 3680.
22. C.P. Yang, Y.X. Yin, H. Ye, K.C. Jiang, J. Zhang and Y.G. Guo, *ACS Appl. Mater. Interfaces*, 6 (2014) 8789.
23. X. Zhou, Y. Xie, Y.F. Deng, X.S. Qin and G.H. Chen, *J. Mater. Chem. A*, 3 (2015) 996.
24. J.L. Zhang, J. Wang, Y.Y. Liu, N. Nie, J.J. Gu, F. Yu and W. Li, *J. Mater. Chem. A*, 3 (2015) 2043.
25. S.L. Yang, M.J. Hu, L.J. Xi, R.G. Ma, Y.C. Dong and C.Y. Chung, *ACS Appl. Mater. Interfaces*, 5 (2013) 8961.
26. E. Avci, *J. Power Sources*, 270 (2014) 142.
27. J.Y. Li, W.L. Yao, S. Martin and D. Vaknin, *Solid State Ionics*, 179 (2008) 2016.
28. Z. Su, Z.W. Lu, X.P. Gao, P.W. Shen, X.J. Liu and J.Q. Wang, *J. Power Sources*, 189 (2009) 411.
29. S.H. Park, Y.K. Sun, K.S. Park, K.S. Nahm, Y.S. Lee and M. Yoshio, *Electrochim. Acta*, 47 (2002) 1721.
30. S.Y. Chung and Y.M. Chiang, *Electrochem. Solid-State Lett.*, 6 (2003) A278.
31. J.C. Zheng, X. Ou, B. Zhang, C. Shen, J.F. Zhang, L. Ming and Y.D. Han, *J. Power Sources*, 268 (2014) 96.
32. C. Miao, P.F. Bai, Q.Q. Jiang, S.Q. Sun and X.Y. Wang, *J. Power Sources*, 246 (2014) 232.

© 2016 The Authors. Published by ESG (www.electrochemsci.org). This article is an open access article distributed under the terms and conditions of the Creative Commons Attribution license (<http://creativecommons.org/licenses/by/4.0/>).